Formation and Decomposition of Hydroxysiliconates in the Gas Phase

Ian H. Krouse† and Paul G. Wenthold*

Department of Chemistry, Purdue University, 560 Oval Drive, West Lafayette, Indiana 47907-2084

Received March 1, 2004

This work describes studies of the formation, structure, and dissociation of hydroxysiliconate ions. Hydroxide adduct ions can be formed in the reaction of halogenated and oxygenated silanes with hydrated hydroxide, $OH^-(H_2O)_n$. Experiments with mass-selected ions indicate that at least two water solvent molecules are required in order to form a hydroxide adduct of fluorotrimethylsilane. Collision-induced dissociation, ion formation, and ion reactivity studies suggest pentavalent siliconate structures for hydroxide adducts of halogenated silanes but solvated siloxides for the oxygenated species. Electronic structure calculations find three types of hydroxide adduct ions, including the hydroxysiliconate and two forms of solvated siloxides. The relative energies of the ions and the barriers that separate them depend on the substituents on the silanes. Empirical modeling of the cross sections for collision-induced dissociation indicates that loss of HF from fluorinated hydroxide adducts occurs through a loose transition state, whereas loss of alkane/arene occurs through a tight transition state at low activation energies.

Silicon is often invoked as a species that readily exhibits hypervalent behavior.[1−12] In particular, it forms pentavalent, trigonal-bipyramidal anions called siliconates, in both the gas[13] and condensed phases.[14−18] Pentavalent siliconate ions have been used in the condensed phase for the investigation of nucleophilic substitution, leading to potential synthetic utility.[14,19−21] Because they are relatively stable, siliconates are often used in fundamental studies of hypervalent bonding.[20,22−25] Siliconates are also good hydride donors[19,23,26−29] and thus have been utilized for the investigation of the stereoselectivity of hydride reduction reactions in the gas phase.[30−32] Consequently, the formation, stability, and decomposition of gaseous siliconates have been investigated both theoretically[33−35] and experimentally.[13,20,36−41]

* To whom correspondence should be addressed. E-mail: pgw@purdue.edu.
† E-mail: krousei@purdue.edu.

(1) Bassindale, A. R.; Glynn, S. J.; Taylor, P. G. In *The Chemistry of Organic Silicon Compounds*; Rappoport, Z., Apeloig, Y., Eds.; Wiley: Chichester, U.K., 1998; Vol. 2, pp 495−511.
(2) Bassindale, A. R.; Taylor, P. G. In *The Chemistry of Functional Groups*; Patai, S., Rappoport, Z., Eds.; Wiley: New York, 1989; Vol. 1, pp 839−892.
(3) Becerra, R.; Walsh, R. In *The Chemistry of Organic Silicon Compounds*; Rappoport, Z., Apeloig, Y., Eds.; Wiley: Chichester, U.K., 1998; Vol. 2, pp 153−180.
(4) Carre, F.; Corriu, R. J. P.; Kpoton, A.; Poirier, M.; Royo, G.; Young, J. C.; Belin, C. *J. Organomet. Chem.* **1994**, *470*, 43−57.
(5) Brefort, J. L.; Corriu, R. J. P.; Guérin, C.; Henner, B. J. L.; Wong Chi Man, W. W. C. *Organometallics* **1990**, *9*, 2080−2085.
(6) Carre, F. H.; Corriu, R. J. P.; Lanneau, G. F.; Yu, Z. F. *Organometallics* **1991**, *10*, 1236−1243.
(7) Chuit, C.; Corriu, R.; Reye, C.; Young, J. C. *Chem. Rev.* **1993**, *93*, 1371−1448.
(8) Corriu, R. J. P.; Young, J. C. In *The Chemistry of Functional Groups*; Patai, S., Rappoport, Z., Eds.; Wiley: New York, 1989; Vol. 1, pp 1241−1288.
(9) Corriu, R. J. P. *J. Organomet. Chem.* **1990**, *400*, 81−106.
(10) Corriu, R.; Guerin, C.; Henner, B. J. L.; Wang, Q. *Organometallics* **1991**, *10*, 3200−3205.
(11) Corriu, R. J. P.; Guérin, C.; Henner, B.; Wang, Q. J. *Organometallics* **1991**, *10*, 2297−2303.
(12) Musher, J. I. *Angew. Chem., Int. Ed. Engl.* **1969**, *8*, 54−68.
(13) DePuy, C. H.; Damrauer, R.; Bowie, J. H.; Sheldon, J. C. *Acc. Chem. Res.* **1987**, *20*, 127−133.
(14) Damrauer, R.; Danahey, S. E. *Organometallics* **1986**, *5*, 1490−1494.
(15) Dixon, D. A.; Farnham, W. B.; Heilemann, W.; Mews, R.; Noltemeyer, M. *Heteroat. Chem.* **1993**, *4*, 287−295.
(16) Marat, R. K.; Janzen, A. F. *Can. J. Chem.* **1977**, *55*, 3845−3849.
(17) Corriu, R. J. P.; Kpoton, A.; Poirier, M.; Royo, G.; Corey, J. Y. *J. Organomet. Chem.* **1984**, *277*, C25−C30.
(18) Johnson, S. E.; Day, R. O.; Holmes, R. R. *Inorg. Chem.* **1989**, *28*, 3183.
(19) Corriu, R. *Pure Appl. Chem.* **1988**, *60*, 99−106.
(20) Damrauer, R.; Burggraf, L. W.; Davis, L. P.; Gordon, M. S. *J. Am. Chem. Soc.* **1988**, *110*, 6601−6606.
(21) Klanberg, F.; Muetterties, E. L. *Inorg. Chem.* **1968**, *7*, 155−160.
(22) Kira, M.; Sato, K.; Sakurai, H. *J. Am. Chem. Soc.* **1988**, *110*, 4599−4602.
(23) Becker, B.; Corriu, R. J. P.; Guérin, C.; Henner, B. J. L. *J. Organomet. Chem.* **1989**, *369*, 147−154.
(24) Hajdasz, D. J.; Squires, R. R. *J. Am. Chem. Soc.* **1986**, *108*, 3139−3140.
(25) Holmes, R. R. *Chem. Rev.* **1990**, *90*, 17−31.
(26) Corriu, R. J. P.; Guérin, C.; Henner, B. J. L.; Wang, Q. *Organometallics* **1991**, *10*, 3574−3581.
(27) Corriu, R.; Guérin, C.; Henner, B.; Wang, Q. *Inorg. Chim. Acta* **1992**, *198*, 705−713.
(28) Chopra, S. K.; Martin, J. C. *J. Am. Chem. Soc.* **1990**, *112*, 5342−5343.
(29) Kira, M.; Kobayashi, M.; Sakurai, H. *Tetrahedron Lett.* **1987**, *28*, 4081−4084.
(30) Ho, Y.; Squires, R. R. *Org. Mass Spectrosc.* **1993**, *28*, 1658−1664.
(31) Hajdasz, D. J.; Ho, Y.; Squires, R. R. *J. Am. Chem. Soc.* **1994**, *116*, 10751−10760.
(32) Artau, A.; Ho, Y.; Kenttämaa, H.; Squires, R. R. *J. Am. Chem. Soc.* **1999**, *121*, 7130−7137.
(33) Gordon, M. S.; Davis, L. P.; Burggraf, L. W.; Damrauer, R. *J. Am. Chem. Soc.* **1986**, *108*, 7889−7893.
(34) Davis, L. P.; Burggraf, L. W.; Gordon, M. S. *J. Am. Chem. Soc.* **1988**, *110*, 3056−3062.
(35) Deiters, J. A.; Holmes, R. R. *J. Am. Chem. Soc.* **1987**, *109*, 1686−1692.

10.1021/om049847k CCC: $27.50
Publication on Web 04/15/2004

Formation of siliconate ions in the gas phase is typically accomplished by one of two methods. In many cases, siliconate ions can be formed by termolecular addition of nucleophiles (including hydride, halides, or alkoxides) to silanes under high-pressure conditions.[13] Alternatively, ions can be generated by "soft transfer" from an ion donor. Thus, whereas alkoxysiliconates can be formed by direct addition of alkoxides to silanes at high pressures,[13,20,36,39] ions such as SiH_5^- can be generated by the reaction of silane with $(C_6H_{13})SiH_4^-$, prepared by addition of hydride to *n*-hexylsilane.[24,31]

Reactions of hydroxide with silanes typically do not lead to formation of pentavalent siliconates but, instead, result in formation of siloxide ions (eq 1).[42,43] By relating

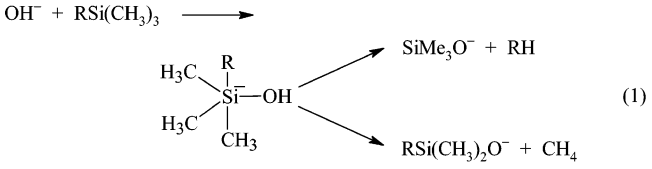

(1)

the branching ratio for siloxide formation to the differences in gas-phase acidities of the resulting neutral molecules, this reaction provides a powerful means for the regioselective measurement of gas-phase acidities and has been applied for the determination of the acidities of alkanes,[42,43] cycloalkanes,[44,45] and arenes.[46−48] However, despite the fact that the reaction is regularly used for thermochemical measurements, the mechanism for siloxide formation from the hydroxysiliconate is not completely understood. A detailed understanding of the mechanism is important if the reaction is to lead to reliable thermochemical data. The proposed mechanism[36,43] for the silane cleavage reaction generally involves addition of hydroxide to form a hydroxysiliconate intermediate, which undergoes competitive elimination to form siloxides (eq 1). DePuy et al.[36] originally suggested that cleavage of RH/CH_4 occurred either through concerted elimination or by stepwise dissociation of R^-, followed by rapid proton transfer. Additional computational[34,39−41] and experimental[13,39,41−44] studies have attempted to differentiate between these two possibilities. It was shown by using deuterium labeling experiments that the cleavage product is formed by deprotonation of the incoming hydroxide,[13,39] but this still allows for either pathway. In 1989, DePuy and co-workers[43] proposed that cleavage of alkanes proceeds through a stepwise process involving formation of a carbanion that is stabilized by solvation of the silanol, followed by rapid deprotonation to give siloxide and methane. Theoretical studies[34] indicated a transition state with substantial negative charge buildup on the departing alkyl group, which was interpreted as being consistent with the mechanism provided by DePuy and co-workers.[36,43] On the basis of RRK/RRKM modeling studies, Wong et al.[41] proposed concerted elimination mechanisms of methane and benzene from pentavalent hydroxysiliconates, with polar transition states similar to those described in the earlier computational work.[34] However, the putative hydroxysiliconate intermediates were not observed in the studies described above, and the decomposition mechanism was deduced from differences between the kinetics of alkoxide photodissociation and those for the reaction of the silane with hydroxide. Although Damrauer and co-workers[20] have reported that hydroxide adduct ions can potentially be formed by the reaction of hydroxide with methoxysilane, or by addition of chloride or fluoride to triethylsilanol, hydroxysiliconates have not been explicitly used to investigate the decomposition reaction.

We recently reported[49] the putative formation of hydroxysiliconate ions of phenyltrifluoro- and phenyltrichlorosilanes by the reaction of these silanes with hydrated hydroxide, $OH^-(H_2O)_n$. In that work, it was shown that collision-induced dissociation (CID) of the hydroxide adduct of phenyltrifluorosilane occurs by competitive loss of HF or benzene (eq 2), whereas the

$$C_6H_5SiF_3OH^- \rightarrow HF + C_6H_5SiF_2O^- \quad (2a)$$

$$\rightarrow C_6H_6 + SiF_3O^- \quad (2b)$$

ion derived from phenyltrichlorosilane loses HCl only. These products are the same as those observed in the reaction of hydroxide with phenyltrifluoro- and phenyltrichlorosilanes, suggesting that they are derived from common hydroxysiliconate intermediates. Attempts to generate the hydroxide adduct of phenyltrimethylsilane by the same approach were unsuccessful.

In this work, we investigate the scope of the reactions of silanes with hydroxide and hydrated hydroxide, with a focus on the formation of hydroxysiliconate ions. By using tandem mass spectrometry, we investigate the role of hydration in the formation of hydroxysiliconate ions, the structures of the hydroxide adducts, and their dissociation mechanisms. Calculations of the structures and dissociation potential energies of the hydroxysiliconates are presented that provide insight into the experimental results. We show experimental and computational evidence that there are at least two types of stable hydroxide adduct ions that can be generated upon reaction of halogenated silanes with hydrated hydroxide, and these ions can interconvert at low energies. We also show that adduct ions can be formed by reaction of hydroxide with oxygenated silanes, but they likely have

(36) DePuy, C. H.; Bierbaum, V. M.; Flippin, L. A.; Grabowski, J. J.; King, G. K.; Schmitt, R. J.; Sullivan, S. A. *J. Am. Chem. Soc.* **1980**, *102*, 5012−5015.
(37) Damrauer, R.; Kass, S. R.; DePuy, C. H. *Organometallics* **1988**, *7*, 637−640.
(38) da Silva, M. L. P.; Riveros, J. M. *J. Mass Spectrom.* **1995**, *30*, 733−740.
(39) Sheldon, J. C.; Hayes, R. N.; Bowie, J. H.; DePuy, C. H. *J. Chem. Soc., Perkin Trans. 2* **1987**, 275−280.
(40) Sheldon, J. C.; Hayes, R. N.; Bowie, J. H. *J. Am. Chem. Soc.* **1984**, *106*, 7711−7715.
(41) Wong, J.; Sannes, K. A.; Johnson, C. E.; Brauman, J. I. *J. Am. Chem. Soc.* **2000**, *122*, 10878−10885.
(42) DePuy, C. H.; Bierbaum, V. M.; Damrauer, R. *J. Am. Chem. Soc.* **1984**, *106*, 4051−4053.
(43) DePuy, C. H.; Gronert, S.; Barlow, S. E.; Bierbaum, V. M.; Damrauer, R. *J. Am. Chem. Soc.* **1989**, *111*, 1968−1973.
(44) Peerboom, R. A. L.; Rademaker, G. J.; de Koning, L. J.; Nibbering, N. M. M. *Rapid Commun. Mass Spectrom.* **1992**, *6*, 394−399.
(45) Broadus, K. M.; Kass, S. R.; Osswald, T.; Prinzbach, H. *J. Am. Chem. Soc.* **2000**, *122*, 10964−10968.
(46) Wenthold, P. G.; Squires, R. R. *J. Mass Spectrom.* **1995**, *30*, 17−24.
(47) Reed, D. R.; Kass, S. R. *J. Mass Spectrom.* **2000**, *35*, 534−539.
(48) Lardin, H. A.; Squires, R. R.; Wenthold, P. G. *J. Mass. Spectrom.* **2001**, *36*, 607−615.
(49) Krouse, I. H.; Lardin, H. A.; Wenthold, P. G. *Int. J. Mass Spectrom.* **2003**, *227*, 303−314.

a solvated siloxide structure. Last, we describe computational and experimental evidence that the dissociation of hydroxysiliconate ions occurs by initial rearrangement to a solvated siloxide, followed by decomposition.

Experimental Section

Instrumental Description and Data Analysis. All gas-phase ion/molecule reactions were carried out using a flowing afterglow−triple-quadrupole mass spectrometer that has been previously described.[50,51] Primary ionic reagents were prepared by 70 eV electron ionization (EI) of neutral precursors and carried by helium buffer gas (0.400 Torr, flow(He) = 190 STP cm^3/s) through the flow tube, where they were allowed to react with neutral vapors added through a micrometering valve. Hydroxide ion was prepared by EI of a 2:1 mixture of methane and nitrous oxide. Hydrated hydroxide was prepared by reaction of hydroxide ion with wet THF.[52,53] Ions generated in the flow tube were sampled through a 1 mm nose cone orifice into a differentially pumped region, where they were analyzed with a triple-quadrupole mass filter (EXTREL). Collision-induced dissociation was carried out by selecting the ion with the desired mass-to-charge ratio with the first quadrupole and injecting the ion into the second quadrupole, q2, which served as a gastight collision cell containing argon as the target gas. The CID collision energy was controlled by the pole offset voltage, and the absolute energy origin was established by using retarding potential analysis. The uncertainty in the absolute energy scale was estimated to be ±0.15 eV in the laboratory frame. Product ions were mass-analyzed with the third quadrupole and detected with a channeltron particle detector operated in pulsed-counting mode.

Cross sections for CID, σ, were calculated using $I/I_0 = \sigma Nl$, where I and I_0 are the intensities of the product and reactant ions, N is the number density of the target, and l is the effective collision path length. The value of l was calibrated to be 24 ± 4 cm[51] by using the reaction of $Ar^+ + D_2$, which has a well-established cross section.[54] Cross sections were measured as a function of target pressure and extrapolated to zero pressure, single-collision conditions.

Cross sections were modeled with the exponential expression shown in eq 3,[55−58] where E is the center-of-mass collision energy of the reactant ion, g_i is the fraction of the ions with internal energy E_i, E_0 is the threshold energy for dissociation, n is a parameter that reflects the energy deposition in the collision,[59] and σ_0 is a scaling factor. The data were modeled

$$\sigma(E) = \sigma_0 \sum_i P_i g_i (E + E_i - E_0)^n / E \qquad (3)$$

by adjusting the parameters to correspond with the steeply rising portion of the appearance curve(s) directly past the threshold. Also convoluted into the fit were the ion kinetic energy distributions, approximated as a Gaussian function with a 1.5 eV (laboratory frame) full-width at half-maximum, and a Doppler broadening function to account for motion of the target. The factor P_i is the probability for ion dissociation, calculated from RRKM theory. Branching ratios for competitive dissociations were calculated from the ratios of rate constants for the competing channels.

Structures of transition states used in the RRKM calculations depend on the type of dissociation that occurs. For direct dissociation reactions, a product-like transition state was assumed, corresponding to the phase-space limit.[60] Structures and frequencies for rearrangement pathways were obtained from electronic structure calculations. Data analysis and modeling were carried out using the CRUNCH 4D program.[54,57,60−62]

Modeled threshold energies, E_0, are 0 K ΔE values and were converted to 298 K bond dissociation enthalpies by using the integrated heat capacities of reactants and products. Uncertainties in enthalpy values were calculated by statistical combination of the uncertainty in the absolute energy scale for the experiment, the standard deviation of values obtained from replicate experimental trials, and uncertainty due to error in the transition state, estimated as the change in the threshold energy that results when the frequencies of the transition state are adjusted to change the activation entropy by ±2 cal/(mol K).

Branching ratio measurements[63,64] were carried out using the flowing afterglow reactor. For these experiments, the yields of relevant ions are measured and plotted with respect to measured flow. Correction of yields involves subtraction of background and adjustment for isotopic distributions. Extrapolation to zero flow gives branching ratios of primary products with an estimated ±5% uncertainty.

Materials. Methane (99.5%) and nitrous oxide (99%) were obtained from BOC gases. Helium gas was purified via a liquid nitrogen trap containing molecular sieves. Fluorotrimethylsilane (96% purity) was purchased from Aldrich and used as received. All other silanes were commercially obtained and distilled under atmospheric conditions prior to use.

Computational Details. Rotational constants and frequencies of reactants, transition states, and products, required to calculate the internal energies of the ion and the RRKM dissociation rates, were calculated at the B3LYP/6-31+G* level of theory[65−75] using Gaussian 98.[76] Geometries, energies, and frequencies of hydroxide adduct structures of fluorotrimethylsilane and the transition states that connect them were also calculated at the B3LYP/aug-cc-pVDZ, B3LYP/aug-cc-

(50) Graul, S. T.; Squires, R. R. *Mass Spectrom. Rev.* **1988**, *7*, 263−358.
(51) Marinelli, P. J.; Paulino, J. A.; Sunderlin, L. S.; Wenthold, P. G.; Poutsma, J. C.; Squires, R. R. *Int. J. Mass Spectrom. Ion Processes* **1994**, *130*, 89−105.
(52) DePuy, C. H.; Beedle, E. C.; Bierbaum, V. M. *J. Am. Chem. Soc.* **1982**, *104*, 6483−6488.
(53) Bickelhaupt, F. M.; de Koning, L. J.; Nibbering, N. M. M. *Tetrahedron* **1993**, *49*, 2077−2092.
(54) Ervin, K. M.; Armentrout, P. B. *J. Chem. Phys.* **1985**, *83*, 166−189.
(55) Chesnavich, W. J.; Bowers, M. T. *J. Phys. Chem.* **1979**, *83*, 900−905.
(56) Ervin, K. M. *Chem. Rev.* **2001**, *101*, 391−444.
(57) Schultz, R. H.; Crellin, K. C.; Armentrout, P. B. *J. Am. Chem. Soc.* **1991**, *113*, 8590−8601.
(58) Sunderlin, L. S.; Armentrout, P. B. *Int. J. Mass Spectrom. Ion Processes* **1989**, *94*, 149−177.
(59) Muntean, F.; Armentrout, P. B. *J. Chem. Phys.* **2001**, *115*, 1213−1228.
(60) Rodgers, M. T.; Ervin, K. M.; Armentrout, P. B. *J. Chem. Phys.* **1997**, *106*, 4499−4508.
(61) Rodgers, M. T.; Armentrout, P. B. *J. Chem. Phys.* **1998**, *109*, 1787−1800.
(62) Dalleska, N. F.; Honma, K.; Sunderlin, L. S.; Armentrout, P. B. *J. Am. Chem. Soc.* **1994**, *116*, 3519−3528.
(63) Adams, N. G.; Smith, D. *J. Phys. B: Atom. Mol. Phys.* **1976**, *9*, 1439−1451.
(64) Grabowski, J. J. In *Studies of Gas-Phase Ion−Molecule Reactions Using a Selected Ion Flow Tube*; University of Colorado: Boulder, Colorado, 1978.
(65) Becke, A. D. *Phys. Rev. A* **1988**, *38*, 3098−3100.
(66) Becke, A. D. *J. Chem. Phys.* **1993**, *98*, 5648−5652.
(67) Lee, C.; Yang, W.; Parr, R. G. *Phys. Rev. B* **1988**, *37*, 785−789.
(68) Miehlich, B.; Savin, A.; Stoll, H.; Preuss, H. *Chem. Phys. Lett.* **1989**, *157*, 200−206.
(69) Ditchfield, R.; Hehre, W. J.; Pople, J. A. *J. Chem. Phys.* **1971**, *54*, 724−728.
(70) Hehre, W. J.; Ditchfield, R.; Pople, J. A. *J. Chem. Phys.* **1972**, *56*, 2257−2261.
(71) Hariharan, P. C.; Pople, J. A. *Theor. Chim. Acta* **1973**, *28*, 213−222.
(72) Hariharan, P. C.; Pople, J. A. *Mol. Phys.* **1974**, *27*, 209−214.
(73) Gordon, M. S. *Chem. Phys. Lett.* **1980**, *76*, 163−168.
(74) Binning Jr., R. C.; Curtiss, L. A. *J. Comput. Chem.* **1990**, *11*, 1206−1216.
(75) Clark, T.; Chandrasekhar, J.; Spitznagel, G. W.; Schleyer, P. v. R. *J. Comput. Chem.* **1983**, *4*, 294−301.

Table 1. Reactivity and Experimental Branching Ratios for Reaction of OH^- and Hydrated OH^- with Various Silanes

silane	branching ratio[a]	OH^- adduct[b] (secondary products)	OH− adduct with $OH^-(H_2O)_n$[c]
$Si(CH_3)_4$	100% $Si(CH_3)_3O^-$	N	N
$C_6H_5Si(CH_3)_3$[d]	100% $Si(CH_3)_3O^-$	N	N
$(CH_3)_3SiNHSi(CH_3)_3$	82% $Si(CH_3)_3O^-$ 18% $(M-1)^-$	N	N
$FSi(CH_3)_3$ (**1**)	32% $Si(CH_3)_3O^-$ 30% $(M-1)^-$ 38% $FSi(CH_3)_2O^-$	N	Y
$C_6H_5SiF_3$ (**3**)	3% SiF_3O^- 75% $C_6H_5SiF_2O^-$ 22% $(M-1)^-$	N	Y
$C_6H_5SiCl_3$	10% Cl^- 25% $C_6H_5SiCl_2O^-$ 65% $(M-1)^-$	N	Y
$Si(CH_3)_3CN$	90% $Si(CH_3)_3O^-$ 10% CN^-	N	Y
$CH_3CH_2OSi(CH_3)_3$ (**2**)	85% $Si(CH_3)_3O^-$ 5% $(M-1)^-$ 10% $CH_3CH_2OSi(CH_3)_2O^-$	Y	Y
$(CH_3)_2CHOSi(CH_3)_3$	2% $(CH_3)_2CHO^-$ 85% $Si(CH_3)_3O^-$ 4% $(M-1)^-$ 9% $(CH_3)_2CHOSi(CH_3)_2O^-$	Y	Y
$C_6H_5OSi(CH_3)_3$	40% $Si(CH_3)_3O^-$ 55% $C_6H_5O^-$ 5% $(M-1)^-$	Y	Y
$CH_3CO_2Si(CH_3)_3$	25% CH_3COO^- 55% $Si(CH_3)_3O^-$ 20% $(M-1)^-$	Y	Y
$(CH_3)_3SiOSi(CH_3)_3$	87% $Si(CH_3)_3O^-$ 8% $(M-1)^-$ 5% $(CH_3)_3SiOSi(CH_3)_2O^-$	Y	Y
$Si(OCH_2CH_3)_4$	100% $(CH_3CH_2O)_3SiO^-$	Y	Y

[a] Flow tube branching ratios for the reaction of OH^- with silane, extrapolated to the single-collision limit. [b] Indicates whether the hydroxide adduct is observed in the reaction of silane with hydroxide under any reaction conditions; hydroxide adducts are not formed as primary products. [c] Indicates whether the hydroxide adduct is observed in the reaction of the silane with hydrated hydroxide; the ions in the flowing afterglow have $n = 0-4$. [d] This branching ratio has been previously reported[43] as 97% $Si(CH_3)_3O^-$ and 3% $C_6H_5Si(CH_3)_2O^-$; however, $C_6H_5Si(CH_3)_2O^-$ was not observed in this work. The difference is likely due to multiplier discrimination.[46]

pVTZ, and MP2/aug-cc-pVDZ levels of theory.[77−82] Single-point energies at the MP2,[83−87] MP4,[88,89] and B3LYP levels of theory were calculated at each of the optimized geometries. Zero-point energy and thermal corrections to single-point energies were calculated from unscaled frequencies obtained at the same level of theory as the geometry.

Results and Discussion

Here we report the results of our studies of the formation, structure, and dissociation of hydroxide adducts of silanes. The first section will describe the formation of hydroxide adducts in the reaction of silanes with hydroxide and hydrated hydroxide and the role of solvation in adduct formation. It also describes the products obtained upon CID of the hydroxide adducts and a comparison with flow tube chemistry. The second section will discuss computational studies of the ion structures, and the last section will consider the mechanism of collision-induced dissociation behavior for the hydroxide adducts in light of the computational predictions. Throughout these sections, the phrase "hydroxide adduct" is used to refer to the addition ion formed in the reaction of the silane plus hydroxide but does not specify the structure of the ion.

Adduct Ion Formation. We have examined the reactivity of the silanes listed in Table 1 with hydroxide and hydrated hydroxide. With bare hydroxide, the main reaction pathways are siloxide formation, direct sub-

(76) Frisch, M. J.; Trucks, G. W.; Schlegel, H. B.; Scuseria, G. E.; Robb, M. A.; Cheeseman, J. R.; Zakrzewski, V. G.; Montgomery, J. A., Jr.; Stratmann, R. E.; Burant, J. C.; Dapprich, S.; Millam, J. M.; Daniels, A. D.; Kudin, K. N.; Strain, M. C.; Farkas, O.; Tomasi, J.; Barone, V.; Cossi, M.; Cammi, R.; Mennucci, B.; Pomelli, C.; Adamo, C.; Clifford, S.; Ochterski, J.; Petersson, G. A.; Ayala, P. Y.; Cui, Q.; Morokuma, K.; Malick, D. K.; Rabuck, A. D.; Raghavachari, K.; Foresman, J. B.; Cioslowski, J.; Ortiz, J. V.; Stefanov, B. B.; Liu, G.; Liashenko, A.; Piskorz, P.; Komaromi, I.; Gomperts, R.; Martin, R. L.; Fox, D. J.; Keith, T.; Al-Laham, M. A.; Peng, C. Y.; Nanayakkara, A.; Gonzalez, C.; Challacombe, M.; Gill, P. M. W.; Johnson, B. G.; Chen, W.; Wong, M. W.; Andres, J. L.; Head-Gordon, M.; Replogle, E. S.; Pople, J. A. *Gaussian 98*, revision A.11.3; Gaussian, Inc.: Pittsburgh, PA, 2002.
(77) Woon, D. E.; Dunning, T. H., Jr. *J. Chem. Phys.* **1993**, *98*, 1358−1371.
(78) Kendall, R. A.; Dunning, T. H., Jr.; Harrison, R. J. *J. Chem. Phys.* **1992**, *96*, 6796−6806.
(79) Dunning, T. H., Jr. *J. Chem. Phys.* **1989**, *90*, 1007−1023.
(80) Peterson, K. A.; Woon, D. E.; Dunning, T. H., Jr. *J. Chem. Phys.* **1994**, *100*, 7410−7415.
(81) Wilson, A.; van Mourik, T.; Dunning, T. H., Jr. *J. Mol. Struct. (THEOCHEM)* **1997**, *388*, 339−349.
(82) Davidson, E. R. *Chem. Phys. Lett.* **1996**, *260*, 514−518.
(83) Head-Gordon, M.; Pople, J. A.; Frisch, M. J. *Chem. Phys. Lett.* **1988**, *153*, 503−506.
(84) Frisch, M. J.; Head-Gordon, M.; Pople, J. A. *Chem. Phys. Lett.* **1990**, *166*, 275−280.
(85) Frisch, M. J.; Head-Gordon, M.; Pople, J. A. *Chem. Phys. Lett.* **1990**, *166*, 281−289.
(86) Head-Gordon, M.; Head-Gordon, T. *Chem. Phys. Lett.* **1994**, *220*, 122−128.
(87) Sæbo, S.; Almlöf, J. *Chem. Phys. Lett.* **1989**, *154*, 83−89.
(88) Krishnan, R.; Pople, J. A. *Int. J. Quantum Chem.* **1978**, *14*, 91−100.
(89) Krishnan, R.; Frisch, M. J.; Pople, J. A. *J. Chem. Phys.* **1980**, *72*, 4244−4245.

stitution, and proton transfer. The products and approximate branching ratios for each of the products are shown in the second column of Table 1. None of the silanes examined in this work form hydroxide adducts as primary products in the reaction with bare hydroxide ion. However, hydroxide adducts are observed as secondary products in the reaction of hydroxide with oxygenated silanes at high silane flow, as indicated in the third column in Table 1. Although we did not examine the reaction of hydroxide with methoxysilane in this work, the results for other oxygenated silanes suggest that the hydroxide adduct observed in the previous study[20] was likely a secondary product. The fourth column in Table 1 indicates whether hydroxide addition is observed as a product in the reaction of hydrated hydroxide with the silane. Adduct ions are observed in the reaction of hydrated hydroxide with the oxygenated and halogenated silanes and cyanotrimethylsilane. Adduct ions are not observed with alkyl- or aryl-substituted silanes, such as tetramethyl- and phenyltrimethylsilane, with either hydroxide or hydrated hydroxide.

The reaction products listed in the second column of Table 1 are also observed when reactions are carried out with hydrated hydroxide. However, they are not necessarily formed in the reaction of the silanes with solvated ions and may result from reaction with bare hydroxide still present in the flow tube. Moreover, given the series of hydrated ions formed in the reaction of OH^- with wet THF ($OH^-(H_2O)_n$, $n = 0-3$), it is not clear from the flow tube chemistry which of the hydrated ions is/are responsible for the formation of the hydroxide addition product. Therefore, we have examined the reactions of hydrated hydroxide ions with fluorotrimethylsilane (($CH_3)_3SiF$ (**1**), *m*/*z* 92) in q2 of the triple-quadrupole analyzer in order to investigate the role of solvation in product formation. As shown in Table 1, the hydroxide adduct of fluorotrimethylsilane is formed in the reaction of the silane with hydrated hydroxide, but not with hydroxide. Mass spectra of the reactions of mass-selected $OH^-(H_2O)_n$ ions ($n = 1-3$) with $(CH_3)_3SiF$ are included as Supporting Information. With $OH^-(H_2O)$, the observed products are *m*/*z* 89, 91, and 93, similar to what is observed in the flow tube in the reaction of the silane with OH^- (Table 1). Very small amounts of products may also be present at *m*/*z* 107 and 111, which likely correspond to hydrated siloxide ions (*m*/*z* 89 and 93). All the observed species have maximum cross sections near 0 eV that drop off substantially at higher energies, indicating that they are formed by exothermic processes. For reactions with $n = 2$ or more, a product is also observed at *m*/*z* 109, corresponding to the hydroxide adduct. The fact that the hydroxide addition product is only observed for hydroxide with two or more solvent molecules is consistent with the hypothesis that the adduct must be formed by soft hydroxide transfer. Moreover, the fact that at least two solvent molecules are required suggests that the reaction with singly hydrated hydroxide is likely too exothermic to allow for adduct formation. If hydroxide transfer from $OH^-(H_2O)$ to the silane is exothermic, then the hydroxide binding energy of the silane is greater than that of water, 26.8 ± 1.0 kcal/mol.[90]

(90) Paul, G. J. C.; Kebarle, P. *J. Phys. Chem.* **1990**, *94*, 5184−5189.

Table 2. Products Obtained upon CID of Hydroxide Adducts of Selected Silanes

silane	CID product[a]
$FSi(CH_3)_3$ (**1**)	**89 ($Si(CH_3)_3O^-$)**, 93 ($FSi(CH_3)_2O^-$)
$CH_3CH_2OSi(CH_3)_3$ (**2**)	89 ($Si(CH_3)_3O^-$)
$C_6H_5SiF_3$ (**3**)	101 (SiF_3O^-), **159 ($C_6H_5SiF_2O^-$)**
$C_6H_5Si^{35}Cl_3$	191 ($C_6H_5Si^{35}Cl_2O^-$)
$Si(CH_3)_3CN$	**26 (CN^-)**, 89 ($Si(CH_3)_3O^-$)
$(CH_3)_2CHOSi(CH_3)_3$	89 ($Si(CH_3)_3O^-$)
$C_6H_5OSi(CH_3)_3$	93 ($C_6H_5O^-$)
$(CH_3)_3SiOSi(CH_3)_3$	89 ($Si(CH_3)_3O^-$)
$CH_3CO_2Si(CH_3)_3$	**59 ($CH_3CO_2^-$)**, 89 ($Si(CH_3)_3O^-$), 131 ($M-1^-$)
$Si(OCH_2CH_3)_4$	179 ($Si(OCH_2CH_3)_3O^-$)[b]

[a] For multiple dissociation channels, the major product is in boldface. [b] CID also gave ions at *m*/*z* 150 and 121 resulting from secondary fragmentation of the *m*/*z* 179 ion.

Ion Dissociation and Ion Structures. The structures of the hydroxide adducts have been examined by using energy-resolved collision-induced dissociation. CID products and the relative yields at 25 eV (lab frame) are listed in Table 2. For the halogenated silanes, the CID products of the hydroxide adducts generally resemble the reaction products listed in Table 1, except that those products resulting from deprotonation are not observed upon CID. These results suggest that siloxide formation and substitution can occur via hydroxide addition to the silane (eq 1) but that proton transfer occurs without the formation of an adduct. The CID behavior of the hydroxide adducts of the oxy-substituted silanes, however, is often different from that of the other derivatives. For example, whereas CID of the hydroxide adduct of **1** leads to the same siloxide products that are observed in the flow tube reaction of **1** and OH^- (eq 4 in Scheme 1), CID of the hydroxide adduct of ethoxytrimethylsilane ($CH_3CH_2OSi(CH_3)_3$ (**2**)) results in formation of trimethylsiloxide by loss of ethanol as the only ionic product, in contrast to the flow tube reaction that gives trimethylsiloxide, ethoxydimethylsiloxide, and the deprotonation product (eq 5 in Scheme 1).[91]

Differences between the flow tube reactivity and hydroxide adduct CID are found for most of the oxy-substituted silanes, whereas the CID behavior of the hydroxide adducts of the halogenated silanes (and cyanotrimethylsilane) generally reflects the flow tube chemistry. Observed differences between CID and flow tube products are interpreted to mean that the hydroxide adduct examined by CID is not the same ion accessed during the flow tube reaction of the silane with hydroxide. Similarly, CID products that reflect those observed in the flow tube reaction show that the reactions likely proceed through a common intermediate. Thus, if it is assumed that siloxide formation in the flow tube proceeds through a hydroxysiliconate as shown in eq 1, then a simple explanation for the observed differences in the CID behavior of the hydroxide adducts for oxy- and halo-substituted silanes is that the hydroxide adducts of halo-substituted silanes have hydroxysiliconate structures, whereas those of the oxy-substituted silanes do not. A comparison of the results in Tables 1 and 2 in light of these interpretations

(91) In principle, siloxide formation in the flow tube from the reaction of ethoxysilane with hydroxide could also occur by β-elimination, without formation of a hydroxide adduct. However, if that is the case, it only serves to further the distinction between the flow tube chemistry and CID processes.

Scheme 1

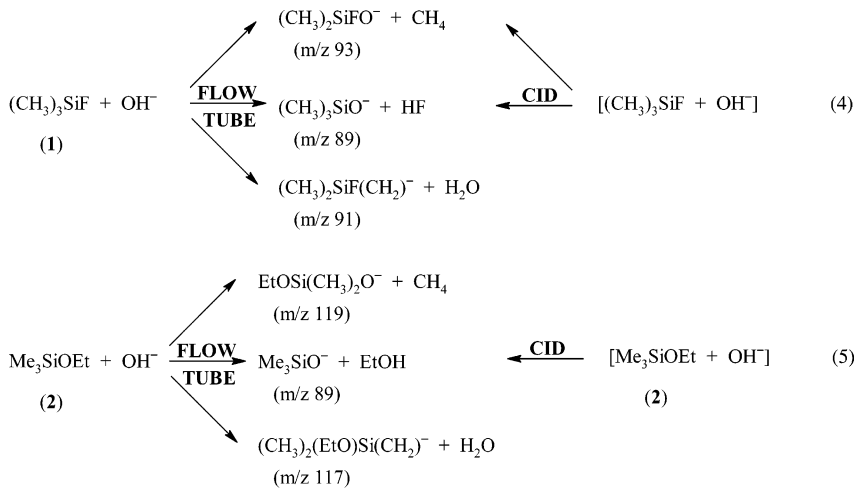

suggests that the hydroxide adducts of $FSi(CH_3)_3$ (**1**) and $C_6H_5SiF_3$ (**3**) have hydroxysiliconate structures, whereas hydroxide adducts of $CH_3CH_2OSi(CH_3)_3$ (**2**), $C_6H_5OSi(CH_3)_3$, and $(CH_3)_2CHOSi(CH_3)_3$ do not.

On the basis of the CID behavior and the computational results described below, the hydroxide adducts of the oxysubstituted silanes are most likely solvated siloxide ions, Me_3SiO^-- - -HOR. To test for this structure, we examined the reaction of the hydroxide adduct of **2** with methanol in the second quadrupole. At low energies, methanol displaces ethanol in the ion, indicating that the ion has a labile ethanol moiety, consistent with a solvated siloxide structure.[92] Methanol does not displace HF in the hydroxide adduct of fluorotrimethylsilane. However, this result does not require a hydroxysiliconate structure for the adduct of **1**, as HF binds to anions more strongly than does methanol.[93]

We also examined the CID behavior of the cluster ions formed in the reaction of trimethylsiloxide ion, $(CH_3)_3SiO^-$, with ethanol and HF (eqs 6a and 6b).

$$(CH_3)_3SiO^- + CH_3CH_2OH \rightarrow (CH_3)_3SiO^-\text{- - -}HOCH_2CH_3 \quad (6a)$$
$$m/z\ 135$$

$$(CH_3)_3SiO^- + HF \rightarrow (CH_3)_3SiO^-\text{- - -}HF \quad (6b)$$
$$m/z\ 109$$

These ions have the same mass-to-charge ratio as the hydroxide adducts of ethoxytrimethylsilane (**2**) and fluorotrimethylsilane (**1**) but are generated by alternate approaches. In both cases, the CID spectra of the resulting ions are indistinguishable from those of the hydroxide adduct ions, suggesting a common reactant ion structure. Thus, CID of the ion formed by HF addition leads to products resulting from loss of HF and CH_4, whereas the ion formed by ethanol addition loses only ethanol. Assuming that the initial step of the reaction involves formation of solvated siloxide, then the result agrees with what is expected for the hydroxide adduct of **2**, for which CID behavior and reactivity suggest a solvated siloxide structure. However, a solvated siloxide structure for the hydroxide adduct of **1** is not consistent with the CID results, which indicate a hydroxysiliconate structure. Electronic structure calculations described in the following section resolve the discrepancy, showing that the hydroxysiliconate and solvated siloxide structures for the hydroxide adduct of fluorotrimethylsilane are comparable in energy and are separated by a small energy barrier and can, therefore, readily interconvert.

Chart 1

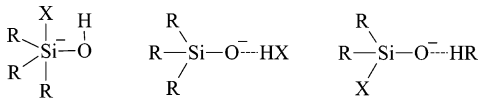

Computational Results. Electronic structure calculations have been used to investigate the structures of the hydroxide adducts examined in this work. This section discusses the relative energies of the hydroxide adduct ions and gives potential energy surfaces that shed light on the mechanism of ion dissociation.

(a) Structures of Hydroxide Adduct Ions of $FSi(CH_3)_3$, $CH_3CH_2OSi(CH_3)_3$, and $C_6H_5SiF_3$. Three distinct low-energy ion structures are identified for the hydroxide adducts, shown in Chart 1. In addition to the hydroxysiliconates labeled as structure **A**, there are also two solvated siloxides. The first siloxide is an alkyl-/aryl-substituted ion solvated by HF or ROH and is labeled structure **B**. The second, structure **C**, is an alkane-/arene-solvated siloxide ion. A silanol-solvated carbanion complex, such as that suggested by DePuy and co-workers,[42] has not been found to be a stable structure for any of the systems investigated in this work. Full geometries, frequencies, Mulliken charges, and absolute energies at the B3LYP/6-31+G* level of theory are provided as Supporting Information. The lowest energy geometries of the hydroxysiliconates, **A**, are trigonal bipyramidal, with the hydroxide substituent equatorial and the electronegative silane substituent (F−, RO−) in the axial position. This allows for hydrogen bonding to occur between the hydroxide and the axial substituent, which is reflected in the lowest energy conformations, as the O−H bond eclipses the axial Si−F

(92) van der Wel, H.; Nibbering, N. M. M.; Sheldon, J. C.; Hayes, R. N.; Bowie, J. H. *J. Am. Chem. Soc.* **1987**, *109*, 5823−5828.

(93) Bartmess, J. E. Negative Ion Energetics Data. In *NIST Chemistry WebBook*; NIST Standard Reference Database 69; Mallard, W. G., Linstrom, P. J., Eds.; National Institute of Standards and Technology: Gaithersburg, MD, 2003 (http://webbook.nist.gov).

Table 3. B3LYP/6-31+G* Relative Energies of Structures A−C for Hydroxide Adduct Ions, Silane Reactants, and Siloxide Products for 1−3[a]

	XR_3SiOH^- (**A**)	R_3SiO^----HX (**B**)	R_2XSiO^----HR (**C**)	$R_3SiX + OH^-$	$R_3SiO^- + HX$
$(CH_3)_3SiF$ (**1**)	0	−6.2	−24.6	42.9	29.3
$CH_3CH_2OSi(CH_3)_3$ (**2**)	0	−13.1	−29.0	35.8	7.0
$C_6H_5SiF_3$ (**3**)	0	4.6	−14.3	74.7	32.8

[a] 298 K enthalpy values in kcal/mol.

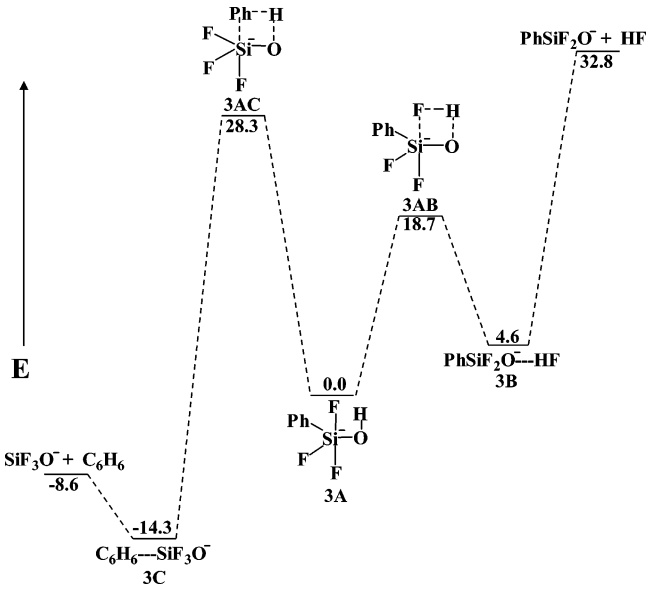

Figure 1. Potential energy diagram for the $C_6H_5SiF_3$ (**3**) + OH^- system with calculated relative enthalpies (B3LYP/6-31+G*).

or Si−O bonds. The geometries in which the hydroxide and electronegative substituent are both axial are typically 1−2 kcal/mol higher in energy, whereas other conformations are ca. 7−8 kcal/mol or more higher in energy. Relative energies are summarized in the Supporting Information.

The relative energies for the lowest energy structures for the three types of ions for three silanes, calculated at the B3LYP/6-31+G* level of theory, are shown in Table 3. The lowest energy isomers for all three systems are the ions with structure **C**, the alkane- or arene-solvated siloxide. For fluorotrimethylsilane (**1**) and ethoxytrimethylsilane (**2**), the solvated siloxides **B** are lower in energy than the hydroxysiliconate ions **A**, but in phenyltrifluorosilane (**3**) the hydroxysiliconate is lower in energy than the solvated siloxide. According to the calculations, the hydroxysiliconate structure is relatively more stable, compared to the solvated siloxide, for systems with more fluoride substituents. The calculated hydroxide affinities of silanes **1**−**3** also increase as more fluorides are added, suggesting that the hydroxide bond energies are related to the relative stabilities of structures **A** and **B** (Table 3, column 5).

(b) Potential Energy Surfaces. Calculations of the critical points along the potential energy surfaces for the dissociation of the hydroxide adducts have been used to investigate the interconversion of the states and the ion dissociation behavior. The general shape of the potential energy surfaces is shown in Figure 1 for phenyltrifluorosilane (**3**). The transition states that connect the three minima described above have been calculated at the B3LYP/6-31+G* level of theory. Thus, the hydroxysiliconate structure **3A** is connected to the HF-solvated siloxide **3B** by transition state **3AB**. Similarly, **3A** is connected to the benzene-solvated siloxide **3C** by transition state **3AC**. The formations of the products from the transition states have been confirmed by calculating the intrinsic reaction coordinate (IRC).[94,95] Ultimately, siloxide formation results by direct dissociation of the solvated siloxides **3B** and **3C**.

The relative energies of all the states on the surface are shown in Figure 1. The key features are the relative energies of the hydroxysiliconate and the HF-solvated siloxide, the heights of the barriers, and the dissociation energy for loss of HF. Although the benzene-solvated siloxide is the lowest energy isomer, the ion binding energy (ca. 6 kcal/mol, Figure 1) is very small; thus, the ion will not be observed in the thermal conditions of flowing afterglow.[13,39] For phenyltrifluorosilane, the hydroxysiliconate is calculated to be lower in energy than the HF-solvated siloxide, such that the ion is predicted to have the hydroxysiliconate structure **3A**, in agreement with the assignment made on the basis of the experimental CID results. Loss of HF from **3A** can occur through the intermediate **3B** and requires ∼33 kcal/mol from the hydroxysiliconate. The energy of the calculated transition state that connects **3A** and **3B** is ca. 14 kcal/mol lower than the dissociation energy to form HF, such that the rate-limiting step for loss of HF should be the dissociation of **3B**. Loss of benzene from **3A** is calculated to be exothermic by 8.6 kcal/mol. As with loss of HF, a stepwise process can occur through intermediate **3C**. However, unlike what is expected for loss of HF, the barrier for loss of benzene is determined by the transition state that connects the hydroxysiliconate with solvated siloxide. The calculated transition states found in this work closely resemble those obtained in previous calculations.[33,41] Most notably, Mulliken charge distributions indicate a significant buildup of charge on the bound atom in the dissociating moiety (see the Supporting Information).

The analogous potential energy surface for the fluorotrimethylsilane system is shown in Figure 2. The main differences from the surface shown in Figure 1 are in the relative energies of the hydroxysiliconate (**1A**) and HF-solvated ion (**1B**) and the height of the barrier that connects them. For fluorotrimethylsilane, the solvated siloxide is calculated to be ca. 6 kcal/mol lower in energy than the hydroxysiliconate, and they are separated by a small energy barrier (∼3 kcal relative to the siliconate). The calculated energy ordering of hydroxysiliconate and solvated siloxide does not agree with that inferred from the experimental CID behavior, which suggested a hydroxysiliconate structure for the ion. Because the

(94) Gonzalez, C.; Schlegel, H. B. *J. Chem. Phys.* **1989**, *90*, 2154−2161.
(95) Gonzalez, C.; Schlegel, H. B. *J. Phys. Chem.* **1990**, *94*, 5523−5527.

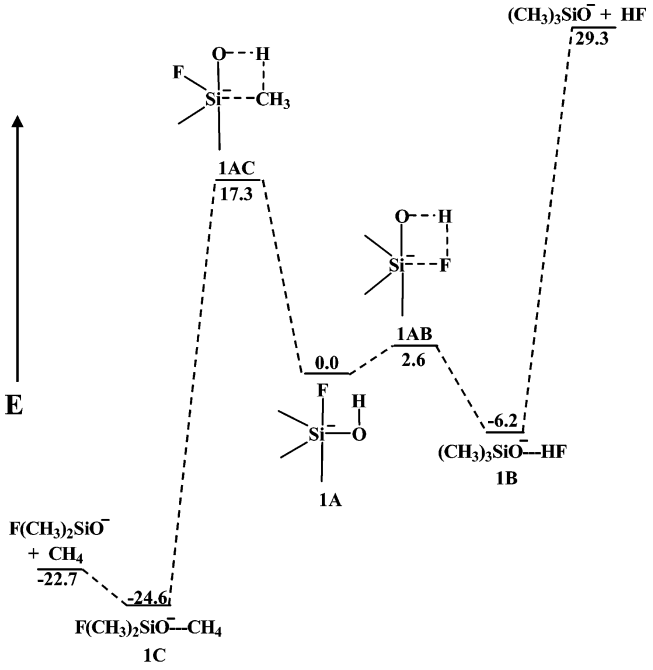

Figure 2. Potential energy diagram for the $(CH_3)_3SiF$ (**1**) + OH^- system with calculated relative enthalpies (B3LYP/6-31+G*).

energies of the ions are fairly close, we have carried out a more thorough computational study of the relative energies of the ions and the transition state. The relative energies, calculated at the B3LYP, MP2, and MP4 levels of theory with Dunning basis sets, are given in Table 4. The solvated siloxide structure is calculated to be lower in energy with most methods, but the energies of the two structures are very close and likely indistinguishable by perturbation theory. Barriers for interconversion of the two structures are generally 2−7 kcal/mol. Thus, although computational studies predict **1B** to be lower in energy, structures **1A** and **1B** are likely close in energy and separated by low energy barriers. Notably, the barrier that connects the ions is much lower than the energies of the reactants used to generate them (**1** + OH^- or Me_3SiO^- + HF; Table 3), such that the lower energy structure can be accessed upon adduct ion formation, accounting for the observation that the CID properties of the adduct ion do not depend on the method by which the ion is formed. The same is true for the hydroxide adduct of phenyltrifluorosilane (Figure 1) and ethoxytrimethylsilane (Figure 3).

The potential energy surface for ethoxytrimethylsilane shown in Figure 3 is significantly different from those for the fluoro-substituted silanes shown in Figures 1 and 2. First, the energy difference between the solvated siloxides **2B** and **2A** is much larger than what was found for **1** or **3**. Therefore, the hydroxide adduct of **2** is predicted to have a solvated siloxide structure, which agrees with the assignment made on the basis of chemical reactivity. Second, the energy for loss of ethanol from structure **2B** is much lower than those for loss of HF from **1B** and **3B**; thus, ethanol loss is much more likely. Thus, loss of ethanol should be the major dissociation pathway, in agreement with the experimental results (Table 2).

Dissociation Mechanism from Energy-Resolved CID Analysis. The mechanisms of dissociation of the

Table 4. Calculated Relative 298 K Energies (kcal/mol) of $FSiMe_3OH^-$ Isomers at Various Levels of Theory

method	$FSi(CH_3)_3OH^-$ (**1A**)	HF loss TS (**1AB**)	$(CH_3)_3SiO^-$---HF (**1B**)
B3LYP/aug-cc-pVDZ Geometry			
B3LYP/aug-cc-pVDZ	0.0	2.5	−5.2
B3LYP/aug-cc-pVTZ[a]	0.0	3.8	−6.3
MP2/aug-cc-pVDZ[a]	0.0	4.4	−1.2
MP2/aug-cc-pVTZ[a]	0.0	4.8	−3.2
MP4/aug-cc-pVDZ[a]	0.0	4.0	−0.3
B3LYP/aug-cc-pVTZ Geometry			
B3LYP/aug-cc-pVTZ	0.0	3.2	−6.2
MP2/aug-cc-pVDZ[a]	0.0	4.2	−0.5
MP2/aug-cc-pVTZ[a]	0.0	5.1	−2.6
MP4/aug-cc-pVDZ[a]	0.0	4.0	0.5
MP2/aug-cc-pVDZ Geometry			
MP2/aug-cc-pVDZ	0.0	4.3	−1.1
B3LYP/aug-cc-pVDZ[a]	0.0	2.2	−4.8
B3LYP/aug-cc-pVTZ[a]	0.0	2.9	−6.3
MP2/aug-cc-pVTZ[a]	0.0	4.9	−2.9
MP4/aug-cc-pVDZ[a]	0.0	4.1	−0.2

[a] Single-point electronic energies based upon the geometries at the indicated levels of theory. Zero-point and thermal energy corrections are obtained by using frequencies calculated at the level of theory used to calculate the geometry.

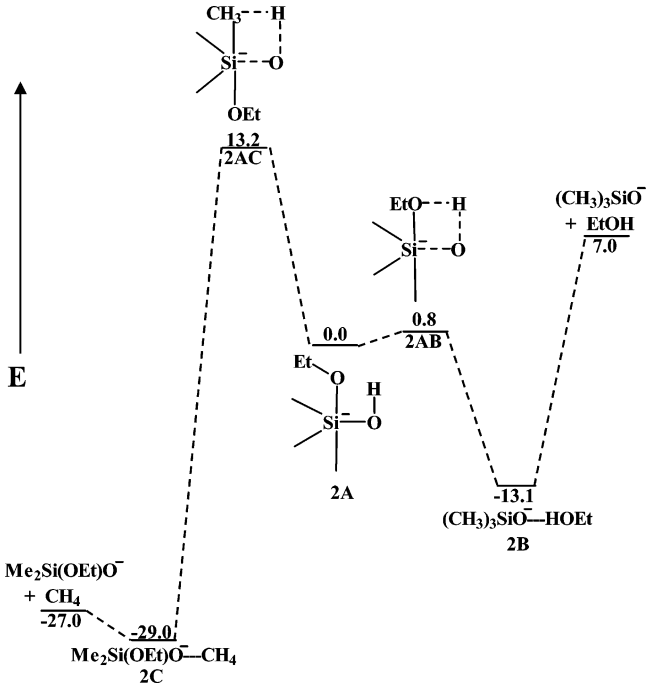

Figure 3. Potential energy diagram for the $CH_3CH_2OSi(CH_3)_3$ (**2**) + OH^- system with calculated relative enthalpies (B3LYP/6-31+G*).

hydroxide adducts of **1** and **3** have been examined in more detail experimentally by using energy-resolved CID. As shown in Table 2, the hydroxide adduct of **1** loses methane and HF to form fluorodimethylsiloxide and trimethylsiloxide, respectively, upon CID (eq 4). The cross sections for methane and HF loss from the hydroxide adduct of **1** in the region from 0 to 6 eV (center-of-mass frame) are shown in Figure 4. At low energies, loss of methane to form fluorodimethylsiloxide is slightly more efficient, but trimethylsiloxide is the dominant product at energies above 2 eV.

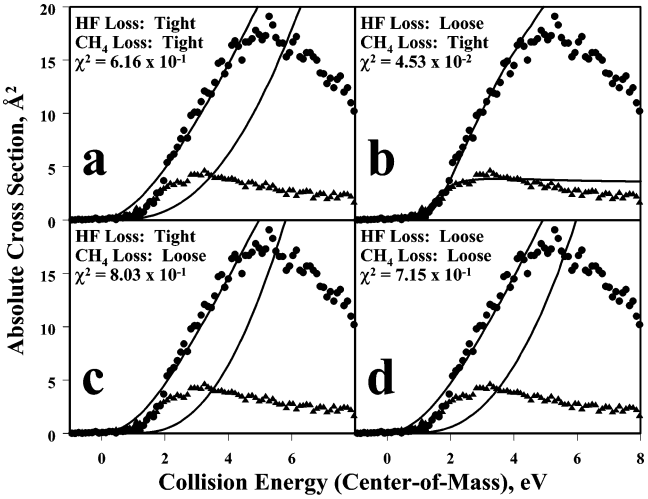

Figure 4. Measured cross-sections for the dissociation of the hydroxide adduct of fluorotrimethylsilane modeled by using various transition state combinations as described in the text. The triangles represent cross sections for loss of methane, and the circles are those for the loss of HF.

Modeling of the energy-resolved cross sections provides insight into the mechanisms of ion dissociation. We have attempted to model the cross sections by using the two types of decomposition mechanisms that have been proposed for the hydroxysiliconate intermediates in the reaction of silanes with hydroxide.[36] The first is a "tight" mechanism involving concerted loss of RH (eq 7). Frequencies for these transition states for concerted

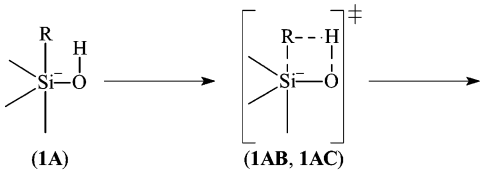

$$RH + Si(CH_3)_3O^- \qquad (7)$$

loss of HF or methane from the hydroxide adduct of **1** are those for the calculated structures **1AB** and **1AC**, respectively. The second is a "loose" mechanism that involves direct dissociation of RH from the solvated siloxide as the rate-limiting step. The frequencies for the loose transition states were approximated from those for the siloxide and RH by using the phase space theory approach described by Rodgers, Ervin, and Armentrout.[60] Parts a−d of Figure 4 show the fits of the cross sections for CID of the hydroxide adduct of fluorotrimethylsilane with different combinations of transition states for product formation. The data in Figure 4 were fit between 1.5 and 3.5 eV, and the reactant ion was assumed to have a hydroxysiliconate structure. Modeling the data by assuming a solvated silioxide structure does not affect the qualitative results but does affect the actual fitting parameters (vide infra).

As can be seen in Figure 4, the best fit to the data is obtained when using a tight transition state for the loss of methane and a loose transition state for the loss of HF. Modeling with the other combinations leads to significantly worse agreement with the data, both visually and statistically (χ^2 value), and does not effectively reproduce the shape of the energy dependence of the methane loss channel. The parameters used to obtain the fit shown in Figure 4b are given in Table 5. From the modeling, it is found that loss of methane has a lower energy barrier than loss of HF but occurs with a tighter transition state and is therefore less efficient at high energies. These conclusions, based solely on the empirical modeling, agree with the computational predictions derived from the potential energy surface shown in Figure 2. With assumption of a solvated siloxide reactant, the measured energy values for loss of HF and methane are 29.5 ± 3.7 and 23.3 ± 3.2 kcal/mol (Figure 2, Table 5), in fair agreement with calculated predictions (Table 3, column 6). Thus, loss of methane has a lower barrier than that for loss of HF and is formed in greater abundance at low energy but has a tighter transition state; therefore, HF loss is preferred at higher energy.

Table 5. Thermochemical Parameters for the CID of Hydroxide Adducts of Fluorotrimethylsilane and Phenyltrifluorosilane[a]

Reactant Ion $FSiMe_3OH^-$ [c]	
barrier for HF loss	31.1 ± 4.2 kcal/mol
barrier for CH_4 loss	25.6 ± 3.7 kcal/mol
n[b]	1.5 ± 0.1
$\Delta S^‡$ (HF loss)	14.8 cal/(mol K)
$\Delta S^‡$ (CH_4 loss)	2.9 cal/(mol·K)
Reactant Ion Me_3SiO^-- - -HF[c]	
barrier for HF loss	29.5 ± 3.7 kcal/mol
barrier for CH_4 loss	23.3 ± 3.2 kcal/mol
n[b]	1.5 ± 0.1
$\Delta S^‡$ (HF loss)	8.3 cal/(mol K)
$\Delta S^‡$ (CH_4 loss)	−2.8 cal/(mol K)
Reactant Ion $C_6H_5SiF_3OH^-$ [d]	
barrier for HF loss	33.4 ± 4.8 kcal/mol
barrier for C_6H_6 loss	38.0 ± 5.3 kcal/mol
n[b]	1.4 ± 0.5
$\Delta S^‡$ (HF loss)	15.6 cal/(mol K)
$\Delta S^‡$ (C_6H_6 loss)	−0.7 cal/(mol K)

[a] Activation barriers correspond to ΔH_{298}. [b] Exponent in eq 3. [c] Data obtained by modeling cross sections for CID of hydroxide adduct of fluorotrimethylsilane. Modeling assumes that loss of HF occurs by a loose transition state, whereas loss of CH_4 occurs by a tight transition state. The reactant ion structure used in the modeling is indicated. The actual structure of the ion (siliconate or solvated siloxide) is not known. [d] Data obtained by modeling low-energy (<3.5 eV) cross sections for CID of the hydroxide adduct of phenyltrifluorosilane. Modeling assumes that loss of HF occurs by a loose transition state, whereas loss of benzene, at threshold, occurs by a tight transition state.

Modeling was also carried out with phenyltrifluorosilane (Figure 5). As with the modeling of the fluorotrimethylsilane data, the cross sections at low energies (<3.5 eV) are best fit when using a loose transition state for loss of HF but a tight transition state for loss of benzene. However, accurate modeling of the data at high energies (>3.5 eV) requires the addition of another benzene loss channel, where the benzene is lost through a loose transition state. Therefore, modeling of the CID data for the hydroxide adduct of phenyltrifluorosilane indicates that the dissociation occurs by a concerted mechanism at low energy but that a pathway with a loose transition state opens at about 3.5 eV. The fully optimized fit for the CID cross sections, obtained with a tight transition state for loss of benzene over the entire range, a direct dissociation channel for loss of benzene above 3.5 eV, and a loose transition state for loss of HF, is shown in Figure 5. The parameters used for the loose transition state for benzene loss at high energy were based upon a dissociation of the ionic leaving group,

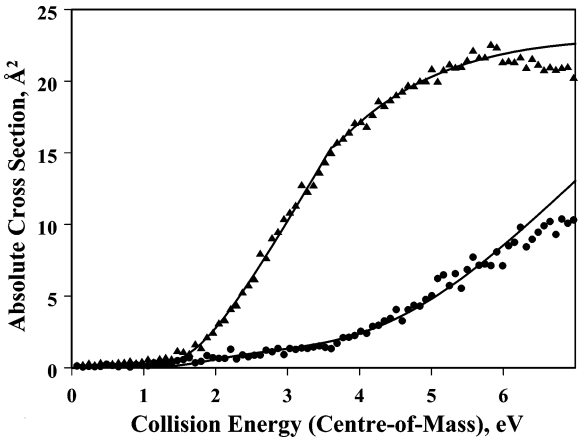

Figure 5. Cross-sections for the dissociation of the hydroxide adduct of phenyltrifluorosilane, and the calculated fit to the data. The circles correspond to loss of benzene, and the triangles represent the pathway corresponding to loss of HF. The benzene loss channel has been multiplied by a factor of 5. The cross section data were modeled using a loose transition state for the loss of HF from 1.5 to 6.2 eV. A tight transition state is used to model the loss of benzene from 1.5 to 6.2 eV and a second, loose transition state from 3.5 to 6.2 eV, as described in the text.

followed by rapid proton abstraction (eq 8), resulting in a stepwise mechanism similar to that proposed by DePuy and co-workers.[36,42,43] Modeling parameters for the low-energy fits of Figure 5 are shown in Table 5.

$$C_6H_5SiF_3OH^- \rightarrow [C_6H_5^- + SiF_3OH] \rightarrow C_6H_6 + SiF_3O^- \quad (8)$$

DePuy and co-workers[36] have previously suggested the possibility of competing loose and tight mechanisms for the dissociation of the fluoride adduct of phenyltrimethylsilane, $(CH_3)_3Si(C_6H_5)F^-$. This agrees with what we have found for the dissociation of $C_6H_5SiF_3OH^-$, where a concerted mechanism is preferred at low activation energies, but the dissociative pathway dominates at higher activation. However, it should be noted that the energy at which the second pathway is observed, 3.5 eV, is higher than the calculated hydroxide affinity of **3** (Table 3). Therefore, it is unlikely that this pathway is accessed during the thermal reaction of OH^- with the silane.

Conclusions

Reactivity and computational studies indicate two distinct stable structures for hydroxide adducts of fluorinated and oxygenated silanes: hydroxysiliconates and solvated siloxides. Alkane-/arene-solvated siloxides are calculated to be the lowest energy structures but are weakly bound with respect to dissociation. The relative energies of hydroxysiliconates and HX-solvated siloxides depend on the substituents, as fluoro-substitution preferentially stabilizes hydroxysiliconate structures. The presence of a low-energy hydroxysiliconate ion is indicated experimentally by CID products that mirror those observed in the gas-phase reaction of OH^- with the silane. The results obtained in this work indicate a hydroxysiliconate as the lowest energy structure for the OH^- adduct of phenyltrifluorosilane but an ethanol-solvated siloxide structure for the product obtained from OH^- with ethoxytrimethylsilane. Experimental and computational studies suggest that the hydroxysiliconate and solvated siloxide structures for the hydroxide adduct of fluorotrimethylsilane are very close in energy and can readily interconvert upon activation.

Modeling of CID cross sections indicates that two types of dissociation mechanisms are possible for hydroxysiliconate ions. Loss of HF from fluorinated hydroxysiliconates is found to occur by a loose mechanism, whereas alkane/arene loss is found to occur by a tight (concerted) transition state at low energies. The results are interpreted in light of computed potential energy surfaces for the hydroxide adducts, which predict the dissociation of hydroxysiliconates to occur by a stepwise mechanism involving rearrangement to the solvated siloxide, followed by decomposition. Whereas the barrier for loss of HF from fluorinated hydroxysiliconate ions is much higher than that for interconversion of the hydroxysiliconate and corresponding solvated siloxide structures, the barrier for loss of alkane/arene is dictated by the energy of the transition state for rearrangement from hydroxysiliconate to solvated siloxide.

The mechanistic insight gained from this and other recent work has important implications for the silane cleavage method of measuring gas-phase acidities. An important assumption in this approach is that the differences in the barriers for the competing alkane-/arene-loss channels mirror the differences in acidities of the leaving hydrocarbon. This assumption is reasonable, assuming a mechanism wherein the rate-limiting step involves cleavage of an anionic leaving group. However, the results of this work, in agreement with the recent studies by Brauman and co-workers,[41] support a more concerted mechanism wherein the barrier is dictated by the energy of the rearrangement transition state and reiterate[41] the call for caution in the use of silane cleavage for measuring acidities. The question of whether it is reasonable to expect the height of the barrier to reflect the acidity of the fragmenting organic moiety is unclear, and studies designed to test the relationship are currently underway.

Acknowledgment. This work was supported by the National Science Foundation (Grant No. CHE-0137627). Thanks also go to the donors of the Petroleum Research Fund, administered by the American Chemical Society, for partial support of this work. We thank Prof. Robert Damrauer for providing unpublished results and insightful discussion.

Supporting Information Available: Figures giving mass spectra of the reaction of $OH^-(H_2O)_n$ with $FSi(CH_3)_3$ for $n = 1-3$ and tables giving conformer energies for hydroxysiliconates of **1**−**3**, Cartesian coordinates, Mulliken charges, unscaled frequencies, and energies for all species **1**, **2**, and **3A**, **B**, **C**, **AB** and **AC**, and Cartesian coordinates, unscaled frequencies, and energies for relevant species used in this work. This material is available free of charge via the Internet at http://pubs.acs.org.

OM049847K